Blast loading on structures

Draganić, Hrvoje; Sigmund, Vladimir

ISSN 1330-3651
UDC/UDK 624.01.04:662.15

BLAST LOADING ON STRUCTURES

Hrvoje Draganić, Vladimir Sigmund

Preliminary notes

The paper describes the process of determining the blast load on structures and provides a numerical example of a fictive structure exposed to this load. The aim was to become familiar with the issue of blast load because of ever growing terrorist threat and the lack of guidelines from national and European regulations on the verification of structures exposed to explosions. The blast load was analytically determined as a pressure-time history and numerical model of the structure was created in SAP2000. The results confirm the initial assumption that it is possible with conventional software to simulate an explosion effects and give a preliminary assessment of the structure.

Keywords: *blast load, conventional software, pressure-time history, terrorist activities, the explosion*

Djelovanje eksplozija na konstrukcije

Prethodno priopćenje

Dana je analiza opterećenja eksplozijom na konstrukciju te numerički primjer djelovanja na fiktivnu građevinu. Cilj je bio upoznati se s fenomenom eksplozije kao opterećenja na konstrukcije uslijed sve veće terorističke prijetnje te nedostatka smjernica u nacionalnim i europskim propisima o provjeri konstrukcija izloženih djelovanju eksplozija. Analitički je određeno opterećenje eksplozijom kao vremenski zapis promjene tlaka zraka te numerički modeliranja konstrukcija i prethodno određeno opterećenje u programskom paketu SAP2000. Dobiveni rezultati potvrđuju početnu pretpostavku kako je moguće konvencionalnim softverom simulirati djelovanje eksplozije i dati preliminarnu ocjenu stanja konstrukcije.

Ključne riječi*: eksplozija, konvencionalni softver, proračunsko opterećenje, terorističke aktivnosti, tlak-vrijeme zapis*

1 Introduction

The terrorist activities and threats have become a growing problem all over the world and protection of the citizens against terrorist acts involves prediction, prevention and mitigation of such events. In the case of structures an effective mitigation may also be thought in the terms of structural resistance and physical integrity. If the structures are properly designed for these abnormal loads damage can be contained. Additionally, in order to ensure safety of existing structures against such events, an evaluation procedure for their inspection and eventual retrofit is needed.

Within the Eurocodes these types of loads are not dealt with (EN 1991-1-7) and they need further elaboration as the engineers have no guidelines on how to design or evaluate structures for the blast phenomenon for which a detailed understanding is required as well as that of the dynamic response of various structural elements. There are no guidelines on such topics. On the other hand, this topic is the interesting one in military circles and important data derived from the experience and tests have been restricted to army use. Nevertheless, a number of publications are available in the public domain and published by the US agencies. Analysis of structures under blast load requires a good understanding of the blast phenomenon and a dynamic response of structural elements. The analysis consists of several steps: (a) estimate of the risk; (b) determination of the computational load according to the estimated hazard; (c) analysis of the structural behaviour; (d) selection of the structural system and (e) evaluation of the structural behaviour.

In this paper we have explored the available literature on blast loads, explained special problems in defining these loads and explored the possibility of vulnerability assessment and risk mitigation of structures with standard structural analysis software with limited non-linear capabilities. It is shown that, with the present knowledge and common software, it is possible to perform the analysis of structures exposed to blast loads and to evaluate their response.

2 Explosions

Explosive is widely used for demolition purposes in: military applications, construction or development works, demolitions, etc. It is, also, a very common terrorist weapon as it is available, easy to produce, compact and with a great power to cause structural damage and injuries. Estimated quantities of explosive in various vehicles are presented in Tab. 1.

Table 1 Estimated quantities of explosives in various vehicles

Vehicle type	Charge mass / kg
Compact car trunk	115
Trunk of a large car	230
Closed van	680
Closed truck	2 270
Truck with a trailer	13 610
Truck with two trailers	27 220

In order to be able to use explosives they have to be inert and stable, which means that the explosion is a triggered, rather than a spontaneous reaction. The explosion is a phenomenon of rapid and abrupt release of energy. Speed of the reaction determines the usefulness of explosive materials that can be condensed, solid or liquid. When they detonate they disintegrate emitting the heat and producing gas. Most of the explosives detonate by a sufficient excitation and convert into a very hot, dense gas under high pressure that presents a source of strong explosive wave. Only about one third of the total chemical energy is released by detonation. The remaining two thirds are released slowly in the blasts as the explosive products mix with the surrounding air and burn.

The explosion effects are presented in a wave of high-intensity that spreads outward from the source to the surrounding air. As the wave propagates, it decreases in strength and speed (Fig. 1).

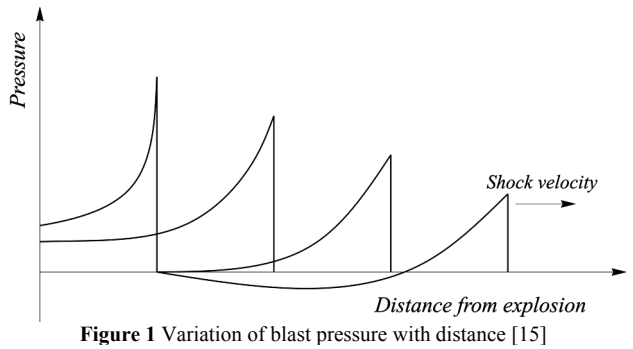

Figure 1 Variation of blast pressure with distance [15]

2.1 Basic parameters of the explosion

Use of the TNT (Trinitrotoluene) as a reference for determining the scaled distance, *Z*, is universal. The first step in quantifying the explosive wave from a source other than the TNT, is to convert the charge mass into an equivalent mass of the TNT. It is performed so that the charge mass of explosive is multiplied by the conversion factor based on the specific energy of the charge and the TNT. Specific energy of different explosive types and their conversion factors to that of the TNT are given in Tab. 2.

Table 2 Conversion factors for explosives

Explosive	Specific energy	TNT equivalent
	Q_x / kJ/kg	Q_x/Q_{TNT}
Compound B (60 % RDX, 40 % TNT)	5190	1,148
RDX (Ciklonit)	5360	1,185
HMX	5680	1,256
Nitroglycerin (liquid)	6700	1,481
TNT	4520	1,000
Explosive gelatin (91 % nitroglycerin, 7,9 % nitrocellulose, 0,9 % antracid, 0,2 % water)	4520	1,000
60 % Nitroglycerin dynamite	2710	0,600
Semtex	5660	1,250
C4	6057	1,340

Explosion wave front speed equation, U_s, and the maximum dynamic pressure, q_s, are defined as [1]:

$$U_s = a_0 \cdot \sqrt{\frac{6p_s + 7p_0}{7p_0}}, \tag{1}$$

$$q_s = \frac{5p_s^2}{2 \cdot (p_s + 7p_0)}, \tag{2}$$

where:

p_s – peak static wave front overpressure, bar
p_0 – ambient air pressure (atmospheric pressure), bar
a_0 – speed of sound in the air, m/s.

There are various proposals for the calculation of the main explosion parameters.

Brode [12] gives the following values for the peak static overpressure for near (when the p_s is greater than 10 bar) and for medium to far away (when the p_s is between 0,1 and 10 bar):

$$p_s = \frac{6,7}{Z^3} + 1, \text{bar}; \quad p_s > 10\,\text{bar} \tag{3}$$

$$p_s = \frac{0,975}{Z} + \frac{1,455}{Z^2} + \frac{5,85}{Z^3} - 0,019, \text{bar} \quad 0,1 < p_s < 10\,\text{bar}, \tag{4}$$

where

Z – scaled distance,

$$Z = \frac{R}{\sqrt[3]{W}}, \tag{5}$$

R – distance from the centre of a spherical charge, m
W – charge mass expressed in kilograms of TNT.

Newmark and Hansen [13] proposed the use of the following values:

$$p_s = 6784 \cdot \frac{W}{R^3} + 93 \cdot \sqrt{\frac{W}{R^3}}, \text{bar} \tag{6}$$

Mills [14] proposed the following:

$$p_s = \frac{1772}{Z^3} + \frac{114}{Z^2} + \frac{108}{Z} - 0,019, \text{kPa}. \tag{7}$$

Other important parameters include: t_0 = duration of the positive phase during which the pressure is greater than the pressure of the surrounding air and i_s = the specific wave impulse that is equal to the area under the pressure-time curve from the moment of arrival, t_A, to the end of the positive phase and is given by expression:

$$i_s = \int_{t_A}^{t_A + t_0} p_s(t)\,\mathrm{d}t. \tag{8}$$

The typical pressure profile of the explosion wave in time for the explosion in the air is given in Fig. 2.

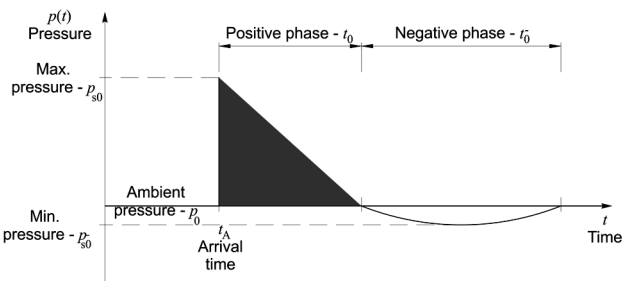

Figure 2 Pressure-time profile of the explosion wave

Where p^- is the maximum value of negative pressure (pressure below ambient pressure) in the negative phase of the blast.

Brode [12] proposed the following value for p^-:

$$p^- = -\frac{0{,}35}{Z}, \text{bar}; Z > 1{,}6. \quad (9)$$

And the corresponding specific impulse at this stage, i_s^-, is given by:

$$i_s^- \approx i_s \cdot \left(1 - \frac{1}{2Z}\right). \quad (10)$$

3 Explosion as a loading

In most instances simplifications lead to conservative constructions. However, unknown factors may lead to the overestimation of the structural capacity to blast loadings. Unexpected shock wave refraction, design methods, quality of construction and materials, interaction with ground, are different for each particular structure. In order to overcome these uncertainties it is recommended that the mass of TNT equivalent is increased by 20 %. This increased value of the charge weight is called the "effective charge weight".

3.1 Loading categories

Explosion loadings can be divided into two main groups according to the confinement of an explosive charge: confined and unconfined. Tab. 3 shows an overview of possible loading categories.

Table 3 Explosion load categories

Charge confinement	Categories
Unconfined	The explosion in the free air
	The explosion in the air
	The explosion near the ground
Confined	Full ventilation
	Partially confined
	Fully confined

3.1.1 Unconfined explosions

The open air explosion causes a wave that spreads from the source of detonation to the structure without any wave amplification. These explosions are situated at a given distance and height away from the structure and there is a wave increase due to the reflection of the ground before it contacts the structure. The height limitations of these explosions are two to three times of the height of a one-story or two-storey structure. The explosion near the ground is an explosion occurring near or on the ground and the initial pressure is immediately increased as a result of refraction on the ground.

3.1.2 Confined explosions

If the explosion occurs inside the structure, the peak pressures associated with the initial wave fronts are extremely high. They are enhanced by the refraction within the structure. In addition to this, depending on the degree of confinement, high temperatures and the accumulation of gaseous products of chemical reactions in the blast would produce more pressure and increase the load duration within the structure. The combined effects of these pressures can lead to the collapse of the structure, if the structure is not designed to withstand internal pressure. Appropriate ventilation reduces strength and duration of pressure so the effect of pressure is different in structures with openings and structures without openings.

3.2 Structure – explosion interaction

As the wave propagates through the air, the wave front encircles the structure and all its surfaces so that the whole structure is exposed to the blast pressure. The magnitude and distribution of the structural loading depends on the following factors:

a) the characteristics of explosives that depend on the type of explosive material, released energy (size of detonation) and weight of explosive,
b) the detonation location relative to the structure,
c) intensity and magnification of pressure in the interaction with the ground or the structure itself.

Time record of the explosion pressure wave is usually described as an exponential function in the form of Friendlander's equation [1], in which the b is the parameter of the waveform:

$$p(t) = p_s \cdot \left(1 - \frac{t}{t_0}\right) \exp\left(-\frac{bt}{t_0}\right). \quad (11)$$

For the various purposes approximations are satisfactory. This change in pressure over time is shown in Fig. 2.

Rankine and Huguenot [1] derived an equation for refracted overpressure p_r:

$$p_r = 2p_s + (\gamma + 1) \cdot q_s. \quad (12)$$

Substituting (2) into the equation (12):

$$p_r = 2p_s \cdot \left(\frac{7p_0 + 4p_s}{7p_0 + p_s}\right). \quad (13)$$

If the rectangular structure is exposed to an explosion, it will be exposed to pressures on all its surfaces. Each surface suffers two concurrent components of the load. Diffraction of explosion around the structure will enclose a target and cause a normal force to any exposed surfaces (Fig. 3). Structure is pushed to the right if the left side is loaded while simultaneously pushed

slightly to the left as the diffraction ends. Drag force pushes the structure from the left side and that is followed by the suction force on the right when the dynamic pressure crosses (blast wind) over and around the structure.

As the shock front expands in surrounding volume of the air, the peak initial pressure is reduced and the duration of the pressure increases.

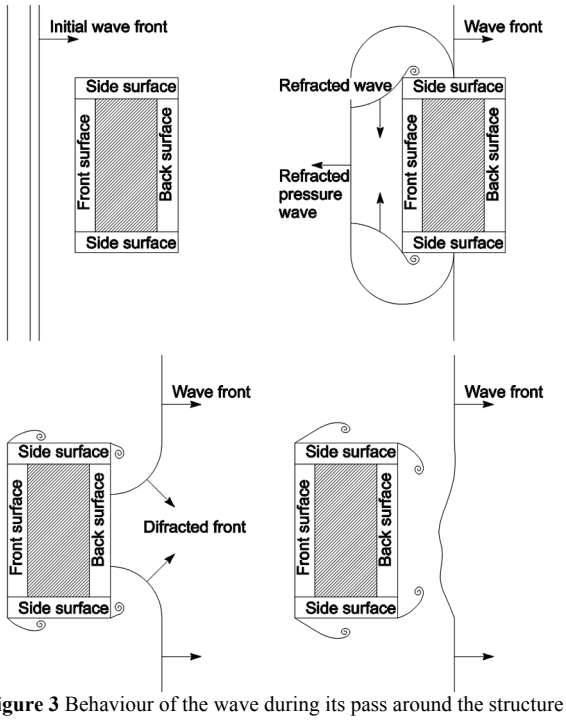

Figure 3 Behaviour of the wave during its pass around the structure

Wave front comes to a particular location at the time t_A, and after the increase to a maximum value of p_{s0}, the peak pressure decreases to the value of atmospheric pressure at the time t_0 what represents a positive phase. This is followed by a negative phase with duration t_0^- which is usually much longer than the positive phase and it is characterized by a negative pressure (below atmospheric) with a maximum value of p_{s0}^- and reverse flow of particles. Impulse associated with the shock wave is the surface below pressure-time curve and is indicated with i_s for the positive phase and i_s^- for a negative phase (Fig. 2).

3.2.1
The explosion in the air

The explosion in the air is a phenomenon that occurs by detonation of explosives above ground level at some distance from the structure so that the blast wave that travels toward the structure is refracted of the ground. The refracted wave is the result of the initial wave amplification by refraction of the ground. Through the front height are occurring variations in pressure, but for the analysis they are ignored, and are regarded as a plane wave across the front height. The parameters are calculated as for an explosion on the ground. Peak refracted pressure $p_{r\alpha}$ is determined using Figs. 2 ÷ 9, from [6] using the scaled charge height above the ground $H_c/W^{1/3}$ and the wave angle α. A similar procedure is applied to determine the impulse $i_{r\alpha}$.

3.2.2
The explosion near the ground

If the charge is located very close to the ground or on the ground the explosion is termed near the ground. Refracted wave arises as the initial blast wave is refracted and increased by reflection of the ground. Unlike an explosion in the air, the refracted wave is merged with the initial wave in the detonation point, and they form a single wave (Fig. 4).

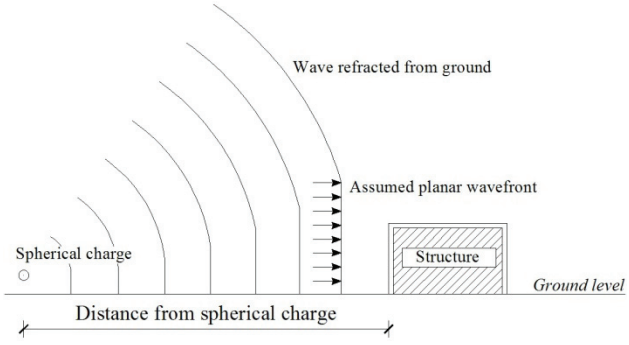

Figure 4 Refracted wave of the explosion near the ground

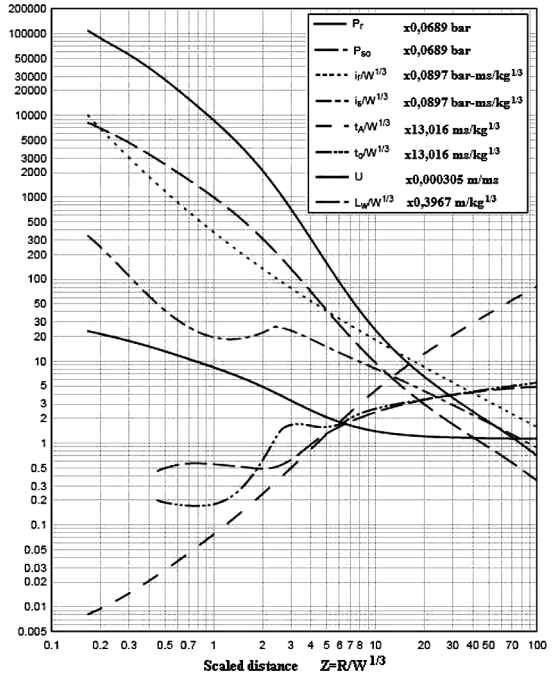

Figure 5 Parameters of the positive phase blast wave near the ground [6]

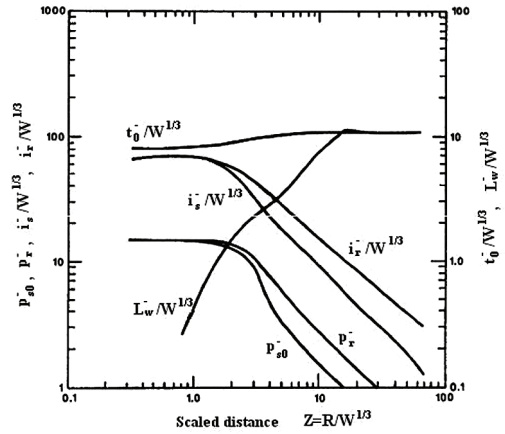

Figure 6 Parameters of the negative phase blast wave near the ground [6]

For an explosion near the ground, the load acting on the structure is calculated as for the explosion in the air, except that the initial pressure and other parameters for the positive phase are determined as explained in Fig. 5 and the theoretical parameters of the negative phase as in Fig. 6.

3.3 Pressures on the structural surfaces

In order to analyze the blast loadings it is necessary to determine the initial reduction of the dynamic pressure in the time as the effects on the structure depend on the pressure-time history as well as on the peak value. The explosion wave form (Fig. 7) is characterized by a sudden increase in pressure to peak, decrease to an atmospheric pressure (positive phase) and the period in which the pressure falls below the atmospheric pressure (negative phase).

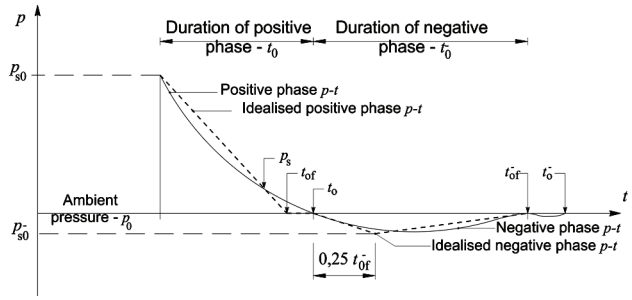

Figure 7 Pressure time history

The reduction speed of the initial and dynamic pressure, after the passing of the wave front, is a function of the peak pressure and the magnitude of detonation. For the analysis purposes, the actual reduction of the initial pressure can be assumed as a triangular pressure impulse. The actual duration of the positive phase is replaced by a fictitious duration and is expressed as a function of the total positive impulse and the peak pressure:

$$t_{of} = \frac{2i}{p}. \tag{14}$$

This expression can be used for the initial and for the refracted pressure by taking the values of refracted impulse pressure and peak refracted pressure, respectively. A similar procedure applies for the values of the negative phase:

$$t_{of}^- = \frac{2i^-}{p^-}. \tag{15}$$

As the fictitious duration of the positive phase is shorter than the actual duration, a difference between the fictitious phase and the beginning of the negative phase is created. This difference, shown in Fig. 7, should be retained in the analysis because of the retention order of the different stages of loading.

3.3.1 The average pressure on the front facade

The variation of the pressure on the front structural facade, for a rectangular structure with sides parallel to the wave front above the ground, in the area of low pressure is shown in Fig. 8.

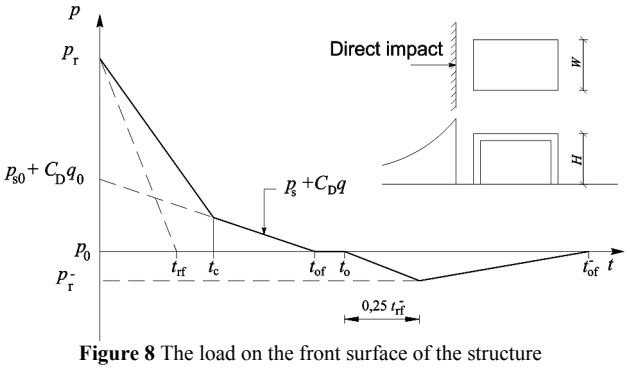

Figure 8 The load on the front surface of the structure

The peak pressure on the front structural facade in time of the explosion's arrival, t_A, will be the peak refracted overpressure p_r, which is a function of the initial pressure (Fig. 5). This pressure then decreases in time interval [t', t_A] due to the passage of waves above and around the structure, which is less than p_r (peak overpressure over and around the structure will be p_s). The overpressure on the front surface of the structure continues to decrease until the pressure is equalized with the pressure of the surrounding air. Clearing time (passing time), t_c, needed that the refracted pressure drops to the level of the initial pressure can be expressed as:

$$t_c = \frac{4S}{(1+R)\cdot C_r}, \tag{16}$$

where:
S – length of the "clearing", is equal to the height of the structure, H or a half-width of the structure, $W/2$, whichever is less (Fig. 8),
R – ratio S/G, where G is the height of the structure, H or half-width of the structure, $W/2$, whichever is less,
C_r – speed of sound in refracted area (Figs. 2 ÷ 192, [6]).

Pressure that acts on the front surface after the time t_c is the algebraic sum of the initial pressure p_s and drag dependent pressure, $C_D \cdot q$:

$$p = p_s + C_D \cdot q. \tag{17}$$

Drag coefficient C_D connects the dynamic pressure and total translational pressure in the direction of the wind-induced dynamic pressure and varies with Mach number (or Reynolds number in the area of low pressure), and depends on the geometry of the structure. It can be taken as ≥ 1,0 for the front facade, while for the side, rear and roof surfaces it can be taken < 1,0 (Tab. 4).

The fictitious length of the refracted wave front, t_{rf}, is calculated according to the formula:

$$t_{rf} = \frac{2i_r}{p_r}, \tag{18}$$

where p_r is the refracted peak pressure.

Table 4 Drag coefficients

Loaded surface	C_D
Front	0,8 ÷ 1,6
Rear	0,25 ÷ 0,5
Side and roof (depending pressure, kN/m^2)	
0 ÷ 172	–0,4
172 ÷ 345	–0,3
345 ÷ 896	–0,2

3.3.2 The average pressure on the roof and side surfaces

As the wave encloses the structure the pressure on the top and sides of the structure is equal to the initial pressure and then decreases to a negative pressure due to the drag (Fig. 9). The structural part that is loaded depends on the magnitude of the initial pressure wave front, the location of the wave front and the wavelength of the positive and negative phases.

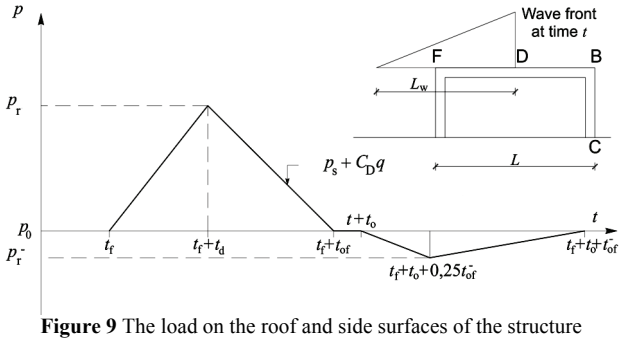

Figure 9 The load on the roof and side surfaces of the structure

The initial peak pressure on the roof surface is reduced and the wavelength increases when the wave encloses the structure. The equivalent uniform pressure increases linearly from the wave-arrival time t_f (point F on the element) to the time t_d when the wave reaches the peak value and gets to the point D. At the point B the equivalent uniform pressure is reduced to zero.

The load coefficient C_E, increase time and duration of an equivalent uniform pressure is determined as explained in Figs. 2 ÷ 196 and 2 ÷ 197 from [6]. It is a ratio of the wavelength and range, L_{wf}/L. The peak pressure that acts on the roof, p_R, is the sum of the equivalent uniform pressure and the drag pressure:

$$p_R = C_E \cdot p_{sof} + C_D \cdot q_0, \tag{19}$$

where are:
p_{sof} – the initial pressure at the point F,
q_0 – a dynamic pressure corresponding to $C_E \cdot p_{sof}$.

The value of the negative pressure that acts on the roof surface, p_R^-, is equal to $C_E^- \cdot p_{sof}$ where C_E^- is the negative value and the equivalent negative pressure t_{of} is determined from Figs 2 ÷ 198, [6]. Time increase of the negative phase is equal to $0{,}25t_{of}$.

3.3.3 The average pressure on the rear surface

As the wave passes over the ends of the roof and side surfaces, pressures are spreading thus creating a secondary wave that continues to spread across the rear surfaces of the structure. The secondary waves that enclose the rear surface, in the case of long structures, are the result of a wave "overflow" from the roof and side surfaces. They are amplified due to the refraction of the structural surfaces. The increase of the waves from the roof is caused by the refraction of the ground at the bottom of the rear surface, and the increase of the waves "overflowed" from the side surface is caused by their mutual collisions in half the length of the surface, or collision with a wave "overflowed" from the roof.

For the loading analysis the procedure equivalent to the procedure for the loading determination on the roof and side surfaces (Fig. 10) can be used. The peak pressure for pressure-time history is determined using the peak pressure on the extreme edge of the roof surface, p_{sob}. Dynamic drag pressure corresponds to the pressure $C_E \cdot p_{sob}$, while the preferred drag coefficients are equal to those for the roof and the side surfaces.

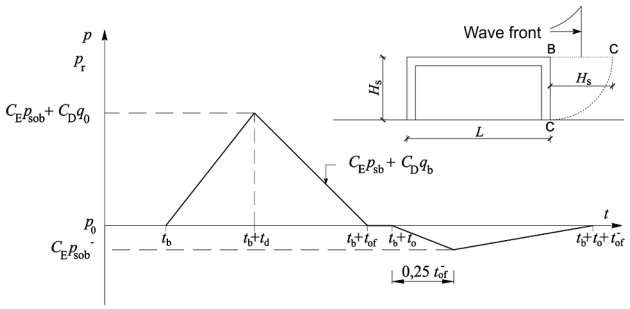

Figure 10 The load on the rear surface of the structure

4 Calculation of the blast loading

For calculating the blast loading on the structural surfaces the following steps are necessary:

Step 1: Determine the weight of the charge, W, charge distance of the structure, R_G, charge height, H_c (for explosions in air) and structural dimensions.

Step 2: Apply safety factor of 20 %.

Step 3: Select several points on the structure (front facade, roof, side and rear surface) and determine the explosion parameters for each selected point.

For the explosion near the ground:

a) Determine the scaled charge distance:

$$Z_G = \frac{R_G}{W^{1/3}},$$

b) Determine the explosion's parameters using Fig. 5 for the calculated scaled distance Z_G and read:
- peak initial positive overpressure p_{s0}
- wave front speed U
- scaled initial positive impulse $i_s/W^{1/3}$
- scaled length of the positive phase $t_0/W^{1/3}$
- scaled value of the wave arrival $t_A/W^{1/3}$.

Multiply the scaled value with the value of $W^{1/3}$ in order to obtain the absolute values.

Step 4: For the front facade:
a) Calculate the peak positive refracted pressure $p_{r\alpha}=C_{r\alpha}\cdot p_{s0}$ and read the coefficient $C_{r\alpha}$ for p_{s0} from Figs 2 ÷ 193, from [6].
b) Read the value of scaled positive refracted impulse $i_{r\alpha}/W^{1/3}$ from Figs. 2 ÷194 (b), from [6] for p_{s0} and α. Multiply the scaled value with the value of $W^{1/3}$ in order to obtain the absolute value.

Step 5: Determine the positive phase of the load on the front facade:
a) Determine the speed of sound in the area of refracted overpressure C_r using Figs. 2 ÷ 192, from [6] for the peak overpressure p_{s0}.
b) Calculate the "clearing" time t_c

$$t_c = \frac{4S}{(1+R)\cdot C_r},$$

c) Calculate the fictitious length of the positive phase t_{of}

$$t_{of} = \frac{2i_s}{p_{s0}}.$$

d) Determine the peak dynamic pressure q_0 from Figs. 2 ÷ 3, from [6] for p_{s0}.
e) Determine $p_{s0} + C_D\cdot q_0$. C_D from Tab. 4.
f) Calculate the fictitious length t_{rf} of the refracted pressure

$$t_{rf} = \frac{2i_{r\alpha}}{p_{r\alpha}}.$$

g) Define the pressure-time history curve for the positive phase. The real load is smaller than the value of impulse pressure due to the refracted pressure (area under the curve) or the purified refracted pressure impulse of the initial pressure.

Step 6: Determine the negative loading phase on the facade. Read the value of Z from Fig. 5 for $p_{r\alpha}$ according to Step 4a) and $i_{r\alpha}/W^{1/3}$ according to Step 4b).
a) Determine $p_{r\alpha}^{-}$ and $i_{r\alpha}^{-}/W^{1/3}$ from Fig. 5 for the value of Z according to Step 6a). Multiply the scaled value of the negative impulse with $W^{1/3}$ in order to obtain an absolute value.
b) Calculate the fictitious duration of negative refracted pressure

$$t_{rf}^{-} = \frac{2i_{r\alpha}^{-}}{p_{r\alpha}}.$$

c) Calculate the negative phase time increase by multiplying the t_{rf}^{-} with 0,25.
d) Define the pressure-time history curve for the negative phase of the load.

Step 7: Determine the positive loading phase on the side surfaces:
a) Determine the ratio of the wavelength and the range of L_{wf}/L.
b) Read the values of C_E, $t_d/W^{1/3}$, $t_{of}/W^{1/3}$ from Figs. 2 ÷ 196, 2 ÷ 193 and 2 ÷ 194(b), from [6] (peak incident overpressure × 0,0689 bar).
c) Read p_R, t_r, t_0.
d) Determine the dynamic pressure q_0 from Figs. 2 ÷ 3 from [6] using p_{s0}.
e) Calculate $p_R = C_E\cdot p_{sof} + C_D\cdot q_0$ and determine the coefficient C_D according to Tab. 4.
f) Define the pressure-time history curve for the positive loading phase.

Step 8: Determine the negative loading phase:
a) Determine the values of C_E^{-} and $t_{of}^{-}/W^{1/3}$ for the value of L_{wf}/L according to Step 7a) from Figs. 2 ÷ 196 and 2 ÷ 198, from [6].
b) Calculate $p_R = C_E\cdot p_{sof}$ i t_{0f}.
c) Calculate the negative phase time increase by multiplying the t_{0f} with 0,25.
d) Define the pressure-time history curve for the negative loading phase.

Step 9: Determine the load on the roof surface by applying the *Steps* for the side surfaces.

Step 10: Determine the load on the rear surface by applying the procedure given for the side surfaces and by assuming that the rear surface is rotated to a horizontal position.

5
The numerical example

The effects of an explosion of spherical charge of TNT of various masses (1 kg, 10 kg, 100 kg) are considered on the multi-storey building. It is located adjacent to the road built within the neighbouring buildings.

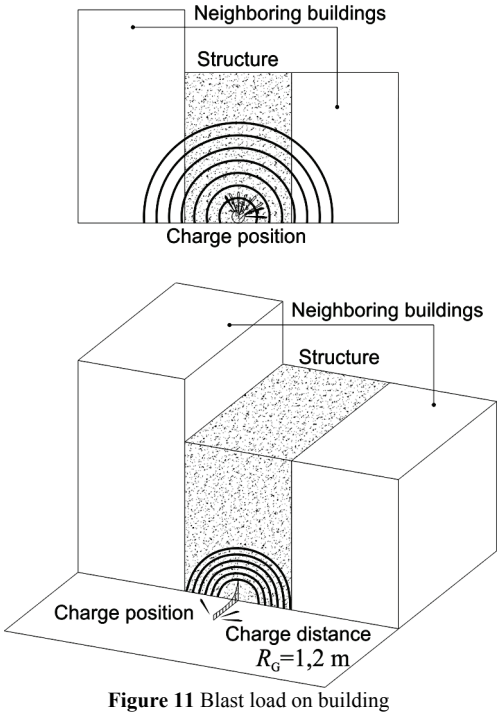

Figure 11 Blast load on building

The example building and its carrying elements are presented in Figs. 11 ÷ 14. It is 16 m long, 17 m wide and 24 m high. Vertical loads are carried by reinforced-concrete slabs that rest on the reinforced-concrete frames. Horizontal loads are carried by mixed frame-wall system with reinforced-concrete walls towards the neighbouring buildings.

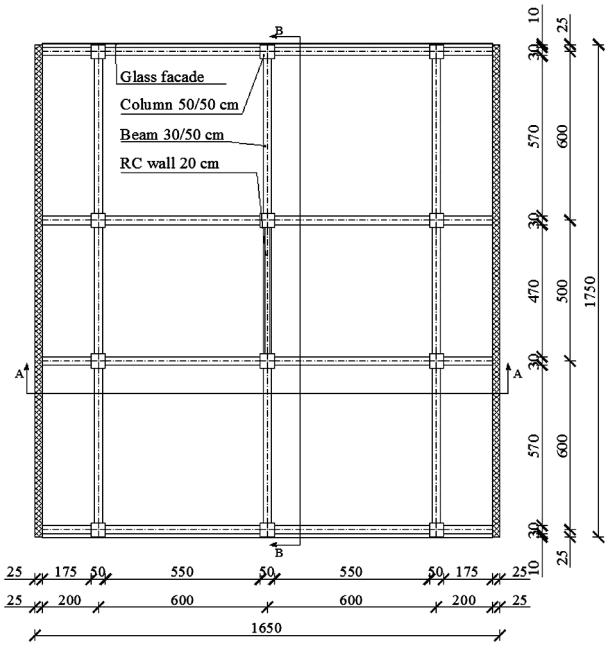

Figure 12 Plan of the building

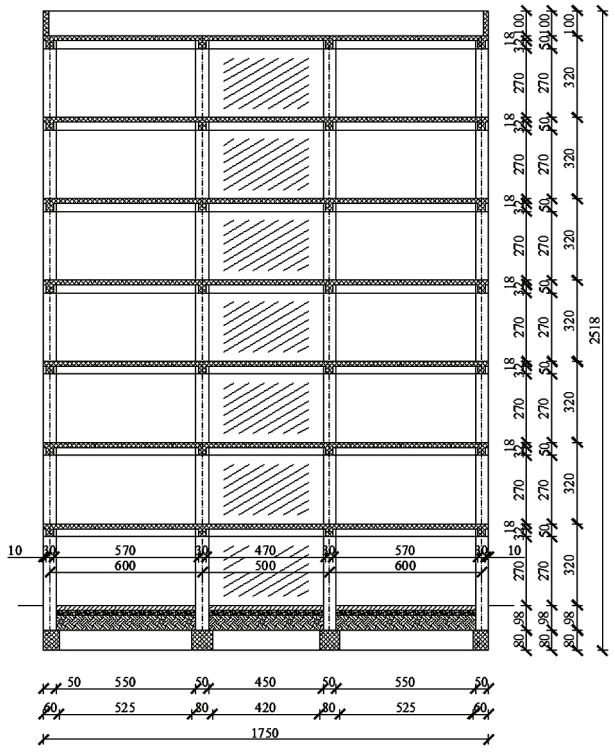

Figure 13 Cross-section A-A

The structure was modelled in the software package SAP2000 v14 as a full 3D model with Beam elements for girders and columns and Shell elements for slabs and walls (Fig. 15). Material nonlinearity is incorporated into the model by using Mander model for concrete (Takeda hysteresis type) and Simple model for steel (Kinematic hysteresis type). The strength of material is increased by including DIF (Dynamic Increase Factor) by a value of 1,25 as recommended in [6]. The analysis included plastic hinges at the columns' and beams' ends in order to observe the plastic behaviour of the structure.

The blast loading is applied only on the front facade as it is surrounded by neighbouring buildings and the explosive charge is located very close to it. The loading on the structure is applied as a pressure-time history of the explosion at certain points. Fig. 16 displays nodal displacement on the front middle structure vertical for three load cases.

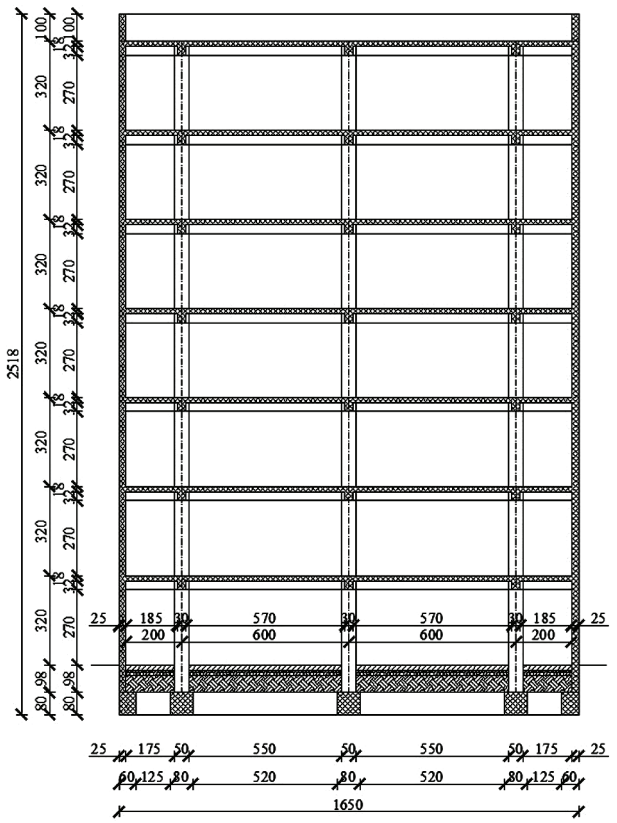

Figure 14 Cross-section A-B

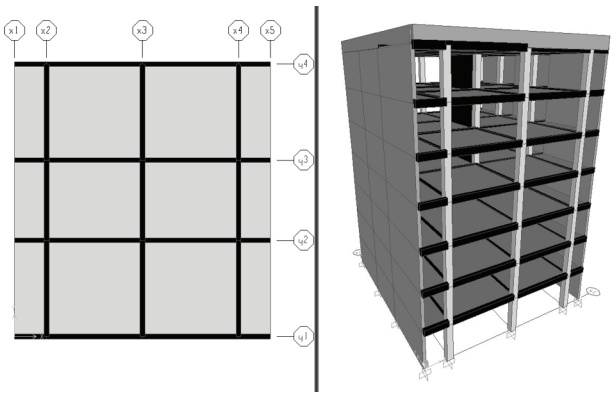

Figure 15 3D structure model in SAP2000

The maximum available deformation of an element is a function of the element length, thickness and type, amount and details of reinforcement used. Its behaviour under blast load depends on the strength and ductility of the element's materials. Control criterion, in the design of blast-resistant structural elements, is the limit on deformation or deflection. In this way the degree of damage sustained by the element may be checked. Damage level that may be tolerated in any particular situation depends on what is to be protected, the structure itself (Protection category 2) or the occupants and equipment (Protection category 1).

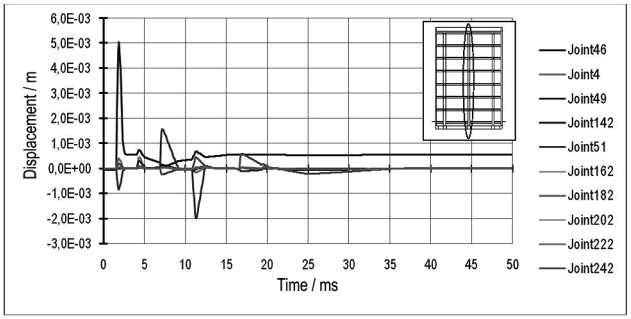

a) 1 kg TNT

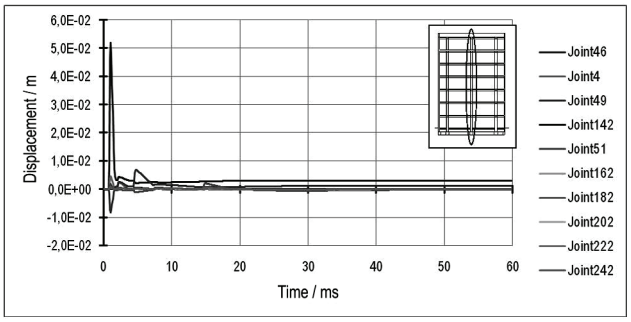

b) 10 kg TNT

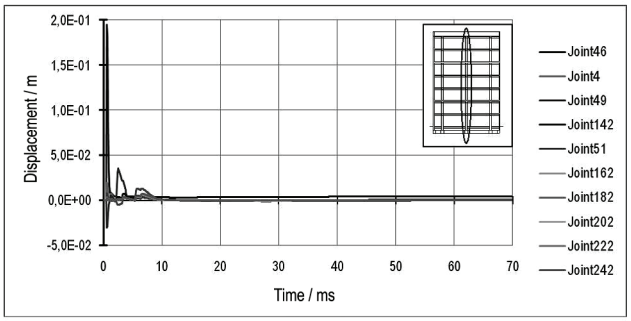

c) 100 kg TNT

Figure 16 Nodal displacement on the front middle structure vertical

There are two methods for specifying the element deformations:

a) Support rotation, θ (Fig. 17):

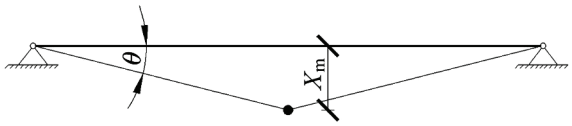

Figure 17 Member support rotation

b) Ductility ratio:

$$\mu = \frac{\text{total deflection}}{\text{deflection at elastic limit}} = \frac{X_{\text{m}}}{X_{\text{E}}}. \qquad (20)$$

Table 5 Protection categories

	Protection categories			
	1		2	
	θ	μ	θ	μ
RC beams and slabs	2°	Not applicable	4°*	Not applicable
Structural steel and plates	2°	10	12°	20
* up to 8° if the element has sufficient lateral resistance to develop tensile membrane action				

Deformations in reinforced concrete elements are expressed in terms of support rotations whilst ductility ratios are usually used for steel elements. These limits (Tab. 5) imply extensive plastic deformation of the elements and need for subsequent repair or replacement before they may be re-used [1].

The results (Tab. 6) indicate, although the source of the explosion is near the structure, that the structure would not collapse. The mass of 100 kg destroyed the middle column. An additional analysis of the structure was made without the middle-ground column destructed by an explosion. It showed the deflection in the place of the removed column of only 5,12 mm. So we conclude that there was a redistribution of load to other elements and that there would be no progressive collapse of the building. However, this should be taken with caution because the analysis of stability of internal structural elements was not carried out.

Table 6 Damage to the columns most exposed to explosion

Charge mass / kg	$\varphi_{j1,C1}$	$\varphi_{j2,C1}$	$\varphi_{j1,C2}$	$\varphi_{j2,C2}$	$\varphi_{d,PC1}$	$\varphi_{d,PC2}$
	degree					
1	0,0044	0,0226	0,1026	0,1632	2,00	5,00
10	0,0539	0,0745	0,8674	1,8231	2,00	5,00
100	0,5901	1,1408	**2,8693**	**5,1921**	2,00	5,00

6 Conclusion

The explosion in or near the structure can cause catastrophic damage to the structure, formation of fragments, destruction of life-support systems (air conditioning, sprinklers). Injuries and deaths can be caused by exposure to explosion wave front, collapse of the structure, impact of parts, fire and smoke. Secondary effects of the explosion can hinder or even prevent the evacuation of people from the structure causing additional injuries and deaths.

Blast load for close explosion was determined and simulated on a model building using SAP2000, the conventional software for the static/dynamic analysis of structures. Loading was defined as a record of pressure over time (pressure-time history) with the parameters calculated by the available literature. Since the model structure was close to the source of detonation, it was not necessary to determine the loading on the structural surfaces, the structure is piecewise loaded. It was necessary to analyze the loading for each point. The aim of the analysis of the structure elements exposed to blast load is to check their demanded ductility and compare it to the available ones. This means that non-liner analysis is necessary and simple plastic hinge behaviour is satisfactory. Deformation history of particular points of interest was calculated and checked against the deformation limits in order to estimate the post-blast state of the element. In elements exposed to distant explosions, conventional reinforcement provides sufficient ductility, while for close explosions additional reinforcement is needed.

The Croatian national legislation and also Euronorms have no guidelines for design of buildings to blast loads. It is shown that the effects of blast loading can be taken into account for structural design by the use of available literature. Available commercial software for structural

analysis can be used for design purposes, while further analysis should be directed towards familiarizing the phenomenon of the internal explosion. Thus a complete picture of the explosion effects on the structure can be obtained.

7 References

[1] Mays, G. C.; Smith, P. D; Blast Effects on Buildings – Design of Buildings to Optimize Resistance to Blast Loading, Tomas Telford, 2001

[2] Ngo, T.; Mendis, P.; Gupta, A.; Ramsay, J. Blast Loading and Effects on Structures – An Overview EJSE Special Issue: Loading on Structures, 2007.

[3] Moon, Nitesh N. Prediction of Blast Loading and its Impact on Buildings, Department of Civil Engineering, National Institute of Technology, Rourkela, 2009.

[4] Remennikov, A. M. A Review of Methods for Predicting Bomb Blast Effects on Buildings. // Journal of Battlefield Technology, Aragon Press Pty Ltd., 6, 3(2003), pp. 5-10.

[5] Đuranović, N. Eksperimentalno modeliranje impulsom opterećenih armiranobetonskih ploča. // Građevinar, 54, 8(2002), pp. 455-463.

[6] Unified Facilities Criteria (UFC), Structures to Resist the Effects of Accidental Explosions, U. S. Army Corps of Engineers, Naval Facilities Engineering Command, Air Force Civil Engineer Support Agency, UFC 3-340-02, 5 December 2008.

[7] van der Meer, L. J. Dynamic response of high-rise building structures to blast load, Research report: A-2008.3, O-2008.8; 2008.

[8] Williamson, E. B.; Bayrak, O.; Williams, G. D.; Davis, C. E.; Marchand, K. A.; McKay, A. E.; Kulicki, J.; Wassef, W. NCHRP Report 645, Blast-Resistant Highway Bridges: Design and Detailing Guidelines, Transportation Research Board, Washington D.C., 2010.

[9] Hameed, A. H. Dynamic Behaviour Of Reinforced Concrete Structures Subjected To External Explosion, A Thesis, Jumada Elawal 1428, 2007.

[10] NEHRP Guidelines for the Seismic Rehabilitation of Buildings (FEMA publication 273), Applied Technology Council (atc-33 project) Redwood City, California, 1997.

[11] FM 3-19.30 (Formerly FM 19.30), Physical Security; Headquarters, Department of the Army, Washington D.C, 2001.

[12] Brode, H. L. Numerical solution of spherical blast waves. // Journal of Applied Physics, American Institute of Physics, Ney York, 1955.

[13] Newmark, N. M.; Hansen, R. J. Design of blast resistant structures. // Shock and Vibration Handbook, Vol. 3, Eds. Harris and Crede. McGraw-Hill, New York, USA. 1961.

[14] Mills, C. A. The design of concrete structure to resist explosions and weapon effects. // Proceedings of the 1st Int. Conference on concrete for hazard protections, Edinburgh, UK, pp. 61-73, 1987.

[15] Ngo, T.; Mendis, P.; Gupta, A.; Ramsay, J. Blast Loading and Blast Effects on Structures – An Overview. // EJSE Special Issue: Loading on Structures (2007).

Authors' addresses

Hrvoje Draganić, dipl. ing. građ.
J. J. Strossmayer University of Osijek
Faculty of Civil Engineering
Crkvena 21, 31000 Osijek, Croatia
e-mail: draganic@gfos.hr

prof. dr. sc. Vladimir Sigmund, dipl. ing. građ.
J. J. Strossmayer University of Osijek
Faculty of Civil Engineering
Crkvena 21, 31000 Osijek, Croatia
e-mail: sigmund@gfos.hr